Particle Accelerators, 1989, Vol. 25, pp. 11-41
Reprints available directly from the publisher
Photocopying permitted by license only

Printed in the United States of America

BEAM BREAKUP WITH COUPLING BETWEEN CAVITIES†

R. L. GLUCKSTERN and F. NERI
Department of Physics, University of Maryland, College Park, MD 20742

(Received November 14, 1988)

We start with the difference equations for *cumulative beam breakup* in a multi-cavity linac structure, modified to include coupling between adjacent cells in the deflecting mode. These equations are solved analytically for small coupling and results are given for the starting current (above which there are runaway oscillations). We obtain approximate universal curves for the starting current as a function of $x = 1/kQ$, where k is the coupling constant and Q the quality factor of the structure. The results are shown to be in excellent agreement with numerical simulations, going over to the previously obtained *cumulative beam breakup* results for large x (small k) and to the *regenerative beam breakup* results for small x (large Q).

I. INTRODUCTION

Beam breakup in a multi-cavity linac occurs when a transverse excitation in one section causes a deflection of the beam, which is then capable of generating or enhancing an excitation in a subsequent section. One extreme case is *cumulative beam breakup*, in which the cavities are assumed to be identical and coupled to one another only by the displacement of beam bunches. In the absence of external focusing, a transient growth of the beam displacement can produce a large magnification of the initial displacement.[1,2] Our analysis has recently been extended[3] to include random fluctuation of parameters such as initial beam displacement, charge per bunch, and the frequency of the dominant transverse mode. In a companion paper, the analysis is extended to include smooth variation of parameters such as the energy, the charge per bunch, the frequency of the dominant transverse mode, and the external focusing force.

At the other extreme, regenerative beam breakup occurs. Here, the cavities are strongly coupled to one another, and the preferred analysis treats the multi-cavity accelerator as a single long tank whose modes of transverse excitation can be represeneted as points on the transverse band of a dispersion curve for a periodic structure. The beam will then interact most strongly with those modes in the transverse band which travel with a phase velocity close to the velocity of the beam. In this model of *regenerative beam breakup*, one mode, in which the phase slip between the beam and this mode is approximately π for the

† Work supported by the U.S. Department of Energy.

transit through the tank, will dominate and lead to instability for beam currents above a "starting current". The model assumes that the modes in the transverse band are well separated from each other.

The object of this paper is to treat the case where the conditions for neither extreme model are present. We assume sufficient electromagnetic coupling between the cavities to make the relative separation between adjacent modes comparable with Q^{-1} (the relative width of each mode). The result of our analysis (which is compared with computer simulations) is then shown to correspond to cumulative beam breakup as the coupling goes to zero and regenerative beam breakup as Q goes to infinity for finite coupling. Finally, we present numerical results which are applicable to the intermediate case, which is often the one encountered in actual multi-cavity accelerators.

II. ANALYSIS

a. Difference Equations Without Coupling

We first review the equations for a coasting beam in the absence of focusing and coupling. The difference equation for the displacement $\xi(N, M)$ of the Mth bunch as it enters the Nth cavity is

$$\xi(N+1, M) - 2\xi(N, M) + \xi(N-1, M) = r\phi(N, M), \tag{II.A.1}$$

where

$$\phi(N, M) = \mathrm{Im}\,[V(N, M)] \tag{II.A.2}$$

and

$$V(N, M) \equiv \sum_{l=0}^{M-1} \xi(N, l) e^{i(M-l)\alpha}, \tag{II.A.3}$$

with

$$\alpha = \omega\tau\left(1 + \frac{i}{2Q}\right). \tag{II.A.4}$$

Here $\omega/2\pi$ and Q are the frequency and quality factor of the deflecting mode, τ is the time interval between bunches, and r is defined as

$$r \equiv \frac{eIc\tau}{2W}\left(\frac{Z_\perp T^2}{LQ}\right)L^2. \tag{II.A.5}$$

Here, r is proportional to the current I and to $Z_\perp/Q$, the ratio of the transverse shunt impedance to the cavity's Q; it is also inversely proportional to the energy W. The cavities, all of length L, are assumed to be touching, and T is the transit time factor. If we change variables from $V(N, M)$ to

$$U(N, M) = e^{-iM\alpha}V(N, M), \tag{II.A.6}$$

Eq. (II.A.3) can be rewritten as

$$U(N, M+1) - U(N, M) = \xi(N, M)e^{-iM\alpha}, \tag{II.A.7}$$

and the difference equation (II.A.1) becomes

$$\delta_N^2[\xi(N, M)] = r \operatorname{Im}[e^{iM\alpha}U(N, M)], \tag{II.A.8}$$

where

$$\delta_N^2(x_N) \equiv x_{N+1} + x_{N-1} - 2x_N. \tag{II.A.9}$$

Equations (II.A.7) and (II.A.8) are the usual equations governing cumulative beam breakup.

b. Field Equation with Coupling/No Beam

Our model for the coupled cavities is a circuit chain with coupling constant k, where the field amplitude in the Nth cavity, $v_N(t)$, satisfies the differential equation

$$\frac{d^2v_N(t)}{dt^2} + \frac{\omega}{Q}\frac{dv_n(t)}{dt} + \omega^2 v_N(t) = -\frac{k\omega^2}{2}[v_{N+1}(t) + v_{N-1}(t)], \tag{II.B.1}$$

where k may be either positive or negative. Changing the variable from $v_N(t)$ to

$$u_N(t) = e^{-i\alpha t/\tau}v_N(t), \tag{II.B.2}$$

and assuming $u_N(t)$ is slowly varying, we find

$$\frac{d}{dt}[u_N(t)] \cong \frac{ik\omega}{4}[u_{N+1}(t) + u_{N-1}(t)], \tag{II.B.3}$$

or

$$\frac{d}{dt}[e^{-i\alpha t/\tau}v_N(t)] \cong \frac{ik\omega}{4}[e^{-i\alpha t/\tau}v_{N+1}(t) + e^{-i\alpha t/\tau}v_{N-1}(t)]. \tag{II.B.4}$$

The independent variable in Eq. (II.B.4) is the time t, which is connected to the cavity number and the bunch number by the relations

$$t = M\tau + NL/c = (M + Ns)\tau, \qquad s = L/c\tau. \tag{II.B.5}$$

On the left side of Eq. (II.B.4) the time derivative at constant N can be replaced by a partial derivative with respect to $M\tau$ (M is considered to be continuous). On the right side, the time in the $(N \pm 1)st$ cavity must correspond to bunch number $M \mp s$. Thus with $v_N(t)$ rewritten as $V(N, M)$ we have

$$\frac{\partial}{\partial M}[V(N, M)e^{-i\alpha(M+Ns)}] \cong$$

$$\frac{ik\omega\tau}{4}[V(N+1, M-s)e^{-i\alpha(M+Ns)} + V(N-1, M+s)e^{-i\alpha(M+Ns)}]. \tag{II.B.6}$$

In terms of the variable $U(N, M)$ defined earlier, we have

$$\frac{\partial U(N, M)}{\partial M} \cong \frac{ik\omega\tau}{4}[U(N+1, M-s)e^{-is\omega\tau} + U(N-1, M+s)e^{is\omega\tau}], \quad \text{(II.B.7)}$$

where we have approximated α by $\omega\tau$ on the right side.

As a final point, we express the group velocity in terms of the coupling constant k. The dispersion curve for mode m in a cavity with N_0 cells is obtained from Eq. (II.B.1) as

$$\omega_m^2 \cong \omega^2[1 + k\cos(m\pi/N_0)] \quad \text{(II.B.8)}$$

The corresponding wave number is $m\pi/N_0L$, from which the group velocity can be obtained as

$$v_g = -k(\omega L/2)\sin(m\pi/N_0). \quad \text{(II.B.9)}$$

Here L is the single cavity length and $m\pi/N_0$ is the phase advance per cavity for mode m. The relevant portion of the dispersion curve for the deflecting band is that for which the phase velocity is equal to c.

c. *Difference/Differential Equations With Beam and Coupling*

It is reasonably straightforward to perform numerical simulations in which the field impulse due to each beam bunch is given by Eq. (II.A.7) and the evolution of the fields between beam bunches is described by Eq. (II.B.1). It is then a simple matter to derive a propagator corresponding to Eq. (II.B.1), with the appropriate boundary conditions for the field in the end cavities. This is in fact the basis for most of the simulations described in this paper.

It is, however, also possible to continue an approximate analysis by combining Eqs. (II.A.7) and (II.B.7). Specifically, we consider the displacement to have rapid oscillations (with frequency $\omega/2\pi$) and write

$$\xi(N, M) = z(N, M)e^{iM\alpha} + z^*(N, M)e^{-iM\alpha *}, \quad \text{(II.C.1)}$$

where $z(N, M)$ and $z^*(N, M)$ are slowly varying functions of N and M. If we neglect rapidly varying terms (valid except near integral values of $\omega\tau/\pi$), Eqs. (II.A.7) and (II.A.8) can be written as

$$U(N, M+1) - U(N, M) \cong z(N, M), \quad \text{(II C.2)}$$

and

$$\delta_N^2 z(N, M) = \frac{r}{2i}U(N, M). \quad \text{(II.C.3)}$$

We now write Eq. (II.B.7) in a centered difference form:

$$U(N, M+s) - U(N, M-s)$$
$$\cong \frac{ik\theta}{2}[U(N+1, M-s)e^{-i\theta} + U(N-1, M+s)e^{i\theta}] + 2sz(N, M-s), \quad \text{(II.C.4)}$$

where

$$\theta \equiv s\omega\tau, \tag{II.C.5}$$

and where we have divided or coalesced the beam bunches so that they are separated in space by $2s\tau c = 2L$. (Our experience with cumulative beam breakup shows that, except near resonance, the variable M can be considered continuous.)

The system of equations (II.C.3), (II.C.4) can be viewed as a single difference equation in the variable M for the $2N_f$-dimensional complex vectors $U(N, M)$, with the appropriate boundary conditions in the first ($N = 1$) and last ($N = N_f$) cavities. It is also possible to treat both M and N as continuous variables to obtain

$$\frac{\partial U}{\partial M} \cong \frac{ik\omega\tau}{4}\left[U(N+1, M-s)e^{-i\theta} + U(N-1, M+s)e^{i\theta}\right] + z(N, M), \tag{II.C.6}$$

and

$$\frac{\partial^2 z(N, M)}{\partial N^2} \cong \frac{r}{2i}U(N, M). \tag{II.C.7}$$

These equations serve together as the starting point for later analysis.

d. Causality

Two methods have been used to determine the starting current numerically. The primary one which is unphysical, uses the Green's function derived from Eq. (II.B.1). For large Q, it can be written as

$$\begin{aligned} G_{ij} &= \sum_{\lambda} \psi_\lambda(i)\psi_\lambda^\dagger(j)\frac{\sin \Omega_\lambda t}{\Omega_\lambda}e^{-\Omega_\lambda t/2Q}, \qquad && t > 0, \\ G_{ij} &= 0, && t < 0. \end{aligned} \tag{II.D.1}$$

Here $\psi_\lambda(i)$ is the ith element of the eigenvector of the matrix operator

$$\Omega^2 = \omega^2\begin{pmatrix} 1 & k/2 & 0 & — & — & — \\ k/2 & 1 & k/2 & — & — & — \\ 0 & k/2 & 1 & — & — & — \\ — & — & — & — & — & — \end{pmatrix} \tag{II.D.2}$$

satisfying

$$\Omega^2\psi_\lambda = \Omega_\lambda^2\psi_\lambda, \tag{II.D.3}$$

with eigenvalue Ω_λ^2.

Note that the formulation in Eq. (II.D.1) does not satisfy causality, since the impulse in cavity i produced by a bunch in cavity j is felt instantaneously for $t > 0$. In other words, Eq. (II.B.1) predicts precursor waves which travel with infinite velocity. An alternate numerical method uses the difference scheme in Eq. (II.C.4), which relates the field in cavity $N - 1$ for bunch $M + s$ to the field in cavity N for bunch $M + s$, corresponding to a signal velocity of $L/s\tau = c$.

Although both schemes give unphysical precursor signals, they lead to the correct dispersion band (frequency ω_b vs phase advance per meter k_b) for the coupled cavity chain. The group velocity $v_g = \partial\omega_b/\partial k_b$ is proportional to the coupling constant k and both schemes lead to no significant energy transport at velocities much larger than v_g.

We therefore expect both schemes to give reliable results as long as k is not large. Here the precursors are unimportant, and numerical tests of each are in good agreement with one another. These schemes, however, are not reliable for large k where the precursor and main signals will be mixed with one another. In this range one needs to use a realistic wakefield derived from Maxwell's equations, but this is beyond the scope of the present paper.

Thus we use the model of Eq. (II.D.1) for numerical calculations of both the starting current and the magnitude of the transient below the starting current.

III. APPROXIMATE FORMULAS FOR STARTING CURRENT

a. Solution to the Differential Equation for Small Coupling and Large N

The solution to Eqs. (II.C.6) and (II.C.7) in the absence of coupling has already been given in an earlier paper.[4] To reiterate: $U(N, M)$ and $z(N, M)$ are assumed to be of the form

$$U(N, M) \cong A \exp[f(M)g(N)], \tag{III.A.1}$$

$$z(N, M) \cong B \exp[f(M)g(N)], \tag{III.A.2}$$

A and B are treated as slowly varying functions of N and M, and derivatives are taken of the exponential only when substituting into Eqs. (II.C.6) and (II.C.7). This leads to the result

$$f(M) = M^{1/3}, \qquad g(N) = \tfrac{3}{2}N^{2/3}r^{1/3}e^{-i\pi/6}. \tag{III.A.3}$$

The real part of the total exponent for $V(N, M)$, including the factor $e^{iM\alpha}$ in Eq. (II.A.6), is[5]

$$e = -\frac{M\omega\tau}{2Q} + \frac{3\sqrt{3}}{4}r^{1/3}N^{2/3}M^{1/3}, \tag{III.A.4}$$

which reaches a maximum value

$$e_0 = (\tfrac{3}{4})^{3/4}N\left(\frac{rQ}{\omega\tau}\right)^{1/2} \tag{III.A.5}$$

at

$$M_0 = (\tfrac{3}{4})^{3/4}Nr^{1/2}(Q/\omega\tau)^{3/2}. \tag{III.A.6}$$

Typical parameters for which beam breakup is serious are small r, large Q and large N, leading to the hierarchy

$$1 \ll e_0 \ll N \ll M_0. \tag{III.A.7}$$

In exploring the behavior for small k, we assume that the hierarchy in Eq. (III.A.7) is still valid, and we approximate $U(N+1, M-s)$ by

$$U(N+1, M-s) \cong U(N, M) + \frac{\partial U(N, M)}{\partial N}. \tag{III.A.8}$$

The validity of Eq. (III.A.8) is based on the expectation from Eq. (III.A.3) that the following order of magnitudes apply:

$$\frac{\partial U}{\partial N} \sim \frac{U}{N} \quad \text{and} \quad \frac{\partial U}{\partial M} \sim \frac{U}{M}.$$

Using Eq. (III.A.8), we can write for Eq. (II.C.6)

$$\frac{\partial U}{\partial M} \cong \frac{ik\omega\tau}{2} \cos\theta\, U + \frac{k\omega\tau \sin\theta}{2} \frac{\partial U}{\partial N} + z. \tag{III.A.9}$$

If we make the substitutions

$$U(N, M) = \tilde{U}(N, M) \exp(ikM\omega\tau \cos\theta/2), \tag{III.A.10}$$

and

$$z(N, M) = \tilde{z}(N, M) \exp(ikM\omega\tau \cos\theta/2), \tag{III.A.11}$$

corresponding to a frequency shift from ω to $\omega(1 + k \cos\theta/2)$, we can write for Eqs. (III.A.9) and (II.C.7):

$$\frac{\partial U}{\partial M} - \varepsilon \frac{\partial U}{\partial N} = \tilde{z} \quad \text{and} \quad \frac{\partial^2 \tilde{z}}{\partial N^2} = \frac{r}{2i} \tilde{U}. \tag{III.A.12}$$

We now change variables from N, M to n, m, with

$$m = M \quad \text{and} \quad n = N + \varepsilon M, \tag{III.A.13}$$

where

$$\varepsilon = k\omega\tau \sin\theta/2. \tag{III.A.14}$$

We then obtain

$$\frac{\partial \tilde{U}}{\partial m} = \tilde{z}, \qquad \frac{\partial^2 \tilde{z}}{\partial n^2} = \frac{r}{2i} \tilde{U}, \tag{III.A.15}$$

which is identical in form to Eqs. (II.C.6) and (II.C.7) for $k = 0$. Thus it appears that the solution for the exponent in Eq. (III.A.4) can be written, with small coupling, as

$$e_k = -\frac{M\omega\tau}{2Q} + \frac{3\sqrt{3}}{4} r^{1/3} M^{1/3} (N + \varepsilon M)^{2/3}, \tag{III.A.16}$$

which, to first power in k (or ε), is

$$e_k \cong -\frac{M\omega\tau}{2Q} + \frac{3\sqrt{3}}{4} r^{1/3} M^{1/3} N^{2/3} + \frac{\sqrt{3}}{2} r^{1/3} M^{4/3} \varepsilon N^{-1/3} \tag{III.A.17}$$

At this point we can make several observations:

(1) Eq. (III.A.17) suggests that beam breakup is enhanced for small positive ε and suppressed for small negative ε. This is confirmed in the simulations, which show that the "starting current" (current above which the displacement grows exponentially with M) is smaller for positive ε than it is for negative ε.

(2) If one assumes that Eq. (III.A.16) is valid for large M, then, in this limit,

$$e_k(\text{large } M) \cong \left(\frac{3\sqrt{3}}{4} r^{1/3}\varepsilon^{2/3} - \frac{\omega\tau}{2Q}\right)M. \tag{III.A.18}$$

This suggests a "starting current" given by

$$r\varepsilon^2 = \frac{8}{81\sqrt{3}}\left(\frac{\omega\tau}{Q}\right)^3, \tag{III.A.19}$$

or, in other terms,

$$\frac{rQ}{\omega\tau} = \frac{32}{81\sqrt{3}}\frac{1}{k^2Q^2\sin^2\theta}. \tag{III.A.20}$$

Surprisingly, this result is the same for positive and negative coupling. As we shall discuss later, it is confirmed in the simulations for positive ε but not for negative ε, for reasons related to the validity of Eq. (III.A.16) for finite N.

(3) We have not applied the boundary conditions on the end cavities in deriving the solutions Eqs. (III.A.16)–(III.A.20). This may explain the fact that the results may not be correct for all values of the parameters. (For our simulations we assume that the fields in cavities $N = 0$ and $N = N_f + 1$ vanish, corresponding to a structure made up of N_f cavities.)

b. Solution to the Difference Equations for Finite N

It is possible to solve Eqs. (II.C.3) and (II.C.4) for the starting current. Specifically, this solution of Eq. (II.C.3) has the correct causal behavior:

$$z(N, M) = \frac{r}{2i}[U(N-1, M) + 2U(N-2, M) + 3U(N-3, M)\cdots], \tag{III.B.1}$$

with $U(0, M) = 0$. If one now tries a solution of the form

$$U(N, M) = e^{pM}U(N), \tag{III.B.2}$$

$$z(N, M) = e^{pM}z(N), \tag{III.B.3}$$

we find

$$\begin{aligned}(e^{2ps} - 1)U(N) = {} & \frac{ik\theta}{2}[e^{-i\theta}U(N-1) + e^{2ps+i\theta}U(N+1)] \\ & + \frac{2sr}{2i}[U(N-1) + 2U(N-2) + 3U(N-3)\cdots].\end{aligned} \tag{III.B.4}$$

The equation for the starting current is then the solution of the corresponding determinantal equation for the homogeneous equations for $U(N)$ given in Eq. (III.B.4). Specifically, the starting current is the value of r for which the determinant vanishes, with

$$\mathrm{Re}\,(p) = \frac{\omega\tau}{2Q}, \tag{III.B.5}$$

since the exponential growth rate for the field and displacement, corresponding to Eqs. (III.B.2), (III.B.3), is

$$\exp\left(-\frac{\omega\tau}{2Q}M + MRe(p)\right). \tag{III.B.6}$$

For small values of $\omega\tau/2Q$, one can expand Eq. (III.B.4) in powers of p, leading to

$$pU(N) \cong \frac{ik\omega\tau}{4}[U(N+1)e^{-i\theta} + U(N-1)e^{i\theta}] + \frac{r}{2i}[U(N-1) + 2U(N-2) + \cdots]. \tag{III.B.7}$$

Changing to the universal variables

$$x \equiv \frac{1}{kQ}, \qquad y \equiv \frac{rQ}{\omega\tau}, \qquad p \equiv -i\frac{\omega\tau}{2Q}q \tag{III.B.8}$$

gives

$$qU(N) + \frac{1}{2x}[U(N+1)e^{-i\theta} + U(N-1)e^{i\theta}] - y[U(N-1) + 2U(N-2) + \cdots] = 0. \tag{III.B.9}$$

For a chain of N_f coupled cavities, the secular determinant of order N_f for Eq. (III.B.9) is

$$D_N \equiv \begin{vmatrix} q & a^* & 0 & 0 & 0 & \cdots \\ a-y & q & a^* & 0 & 0 & \cdots \\ -2y & a-y & q & a^* & 0 & \cdots \\ -3y & -2y & a-y & q & a^* & \cdots \\ \vdots & \vdots & \vdots & \vdots & \vdots & \vdots \end{vmatrix} = 0, \tag{III.N.10}$$

where we have implicitly set $U(0, M)$ equal to $U(N_f + 1, M) = 0$. Here

$$a = \frac{e^{i\theta}}{2x}, \qquad a^* = \frac{e^{-i\theta}}{2x}, \tag{III.B.11}$$

and the starting current is the smallest real value of y for which the solution to Eq. (III.B.10) has

$$\mathrm{Im}\,(q) = 1. \tag{III.B.12}$$

Clearly the solution will be a universal curve giving $y = (rQ/\omega\tau)$ as a function of $x = (1/kQ)$ for different N, as in Eq. (III.A.20).

The $N \times N$ determinant can be expanded by minors to write the recurrence relation

$$D_N - qD_{N-1} + aa^* D_{N-2} = y[a^* D_{N-2} - 2a^{*2} D_{N-3} + 3a^{*3} D_{N-4} \cdots]. \quad \text{(III.B.13)}$$

Equation (III.B.13) can be considered as a recurrence relation with

$$\begin{aligned} D_N &= 0, \qquad N < 0 \\ D_0 &= 1, \qquad D_1 = q, \end{aligned} \quad \text{(III.B.14)}$$

from which one readily finds D_N for $N \geq 2$.

c. *Solution for Two Cavities*

The solution to $D_{N_f} = 0$ for two cavities ($N_f = 2$) is

$$D_2 = q^2 - (aa^* - a^* y) = 0, \quad \text{(III.C.1)}$$

leading to

$$q = \left(\frac{1}{4x^2} - \frac{y}{2x} e^{-i\theta}\right)^{1/2} = u + iv, \quad \text{(III.C.2)}$$

where

$$u^2 - v^2 = \frac{1}{4x^2} - \frac{y}{2x} \cos\theta, \qquad 2uv = \frac{y}{2x} \sin\theta. \quad \text{(III.C.3)}$$

The starting current condition, $v = 1$, leads us to

$$4u^2 = \frac{y^2}{4x^2} \sin^2\theta = \frac{1}{x^2} - \frac{2y}{x} \cos\theta + 4, \quad \text{(III.C.4)}$$

whose solution is

$$y = \frac{-4x \cos\theta \pm (16x^2 + 4\sin^2\theta)^{1/2}}{\sin^2\theta} \quad \text{(III.C.5)}$$

The asymptotes for the hyperbola in Eq. (III.C.5) are

$$y_{\pm\infty}^{(2)} = \frac{4|x|}{1 \pm \cos\theta}, \quad \text{(III.C.6)}$$

and the simulation for $N = 2$ suggests that the $\pm$ sign in the denominator must correspond to the sign of k.

d. *Solution for Several Cavities*

The solution to $D_{N_f} = 0$ for $N_f \geq 3$ involves the roots of an $N_f th$-order algebraic equation. It is possible to obtain the asymptotes for general N_f by recognizing in Eq. (III.B.13) that $a^* \to 0$ and ya^* remain finite as $|x| \to \infty$. Equation (III.B.13) then reduces to

$$D_N - qD_{N-1} - ya^* D_{N-2} = 0, \quad \text{(III.D.1)}$$

which has the general solution, satisfying Eq. (III.B.14),

$$D_N = \frac{z_1^{N+1} - z_2^{N+1}}{z_1 - z_2}, \tag{III.D.2}$$

where

$$z_{1,2} = q/2 + (q^2/4 + a^* y)^{1/2} \tag{III.D.3}$$

The lowest root of $D_N = 0$ is

$$\frac{z_1}{z_2} = e^{2i\pi/(N+1)}, \tag{III.D.4}$$

which is equivalent to

$$q = \left(\frac{2y}{x}\right)^{1/2} e^{i(\pi-\theta/2)} \cos\frac{\pi}{N+1} = \left(\frac{2y}{-x}\right)^{1/2} e^{-(i\theta/2)} \cos\left(\frac{\pi}{N+1}\right), \tag{III.D.5}$$

where the second form is to be used for negative k (or x). The condition $\mathrm{Im}\,(q) = 1$ then gives

$$\left(\frac{2y}{x}\right)^{1/2} = \left\{ \begin{array}{ll} \dfrac{1}{\cos\left(\dfrac{\pi}{N+1}\right)\cos\dfrac{\theta}{2}}, & x > 0 \\ \dfrac{1}{\cos\left(\dfrac{\pi}{N+1}\right)\sin\dfrac{\theta}{2}}, & x < 0 \end{array} \right\} \tag{III.D.6}$$

from which we can write

$$y \cong \frac{|x|\left(1 + \tan^2\dfrac{\pi}{N+1}\right)}{1 \pm \cos\theta} \quad \text{for } x \gtrless 0. \tag{III.D.7}$$

It is also possible to extract the associated intercept for the linear relation in Eq. (III.D.7). This term comes from Eq. (III.B.13) by adding

$$-2a^{*2} y D_{N-3} \tag{III.D.8}$$

to the right side of Eq. (III.D.1). One now treats this term as a perturbation and constructs a Green's function from z_1^N, z_2^N, the solutions to Eq. (III.D.1). The integral of this Green's function multiplied by the perturbing term in Eq. (III.D.8), with D_{N-3} given by its unperturbed value in Eq. (III.D.3), leads to the final relation for the asymptotes

$$y \cong \frac{\left(1 + \tan^2\dfrac{\pi}{N_f+1}\right)}{1 \pm \cos\theta}\left[|x| \mp 2\sin\theta\frac{\left(1 + N_f\cos\dfrac{2\pi}{N_f+1}\right)}{(1+N_f)}\right] \quad \text{for} \quad x \gtrless 0. \tag{III.D.9}$$

It should be noted that Eq. (III.D.9) reduces to Eq. (III.C.6) for $N_f = 2$.

The validity of Eq. (III.D.9) depends on $|a^*| \ll 1$, since, for large $|x|$, $|a^*y|$, q, and D_N are all of the first order. Equation (III.B.11) requires that $|x| \gg 1$ here The quadratic form in Eq. (III.A.20), which can be rewritten as

$$y = \frac{32}{81\sqrt{3}} \frac{x^2}{\sin^2 \theta}, \tag{III.D.10}$$

is therefore expected to be valid for $|x| < 1$, and the transition from Eq. (III.D.10) to Eq. (III.D.9) should take place for $|x|$ of order one. This is confirmed in the simulations, and will be discussed later.

e. Validity of Quadratic Behavior for Large N

Simulations show that the quadratic behavior for y against x in Eq. (III.A.20) is valid for $\varepsilon > 0$, but does not appear to be valid or $\varepsilon < 0$. The reason for this is discussed in Appendix A.

IV. REGENERATIVE BEAM BREAKUP LIMIT

a. Model and Assumptions

The concept of *regenerative beam breakup* involves the interaction of a beam with the transverse modes of a long cavity. In particular, if the cavity is excited in a transverse mode, a beam on axis will be deflected in its transit through the cavity. As the beam moves off axis, it couples to, and can either take energy from that mode or give energy to it. The change in field amplitude from one beam bunch to the next is proportional to the bunch charge as well as the existing field amplitude. In addition, the field amplitude will be decreased (due to the wall loss) by an amount proportional to the field amplitude and to the inverse of the quality factor Q. There is therefore a "starting current" above which the increase due to the beam bunch exceeds the decrease due to wall losses.

The analysis corresponding to the preceding description[6] assumes the excitation of a single mode which travels with a phase velocity close to the velocity of the beam bunches. The relative parameters can be understood by examining the dispersion curves in Fig. 1, drawn for π-mode acceleration in a tank of $N_f = 5$ coupled cavities. The slope of the line OA is proportional to the velocity of the beam bunch. The result of the analysis, expressed in terms of our parameters, is the starting current

$$y = \frac{\pi^3}{2N_f^2 g(\psi)}, \tag{IV.A.1}$$

where

$$g(\psi) = \frac{\pi^3}{2} \frac{1 - \cos\psi - \frac{\psi}{2}\sin\psi}{\psi^3} \tag{IV.A.2}$$

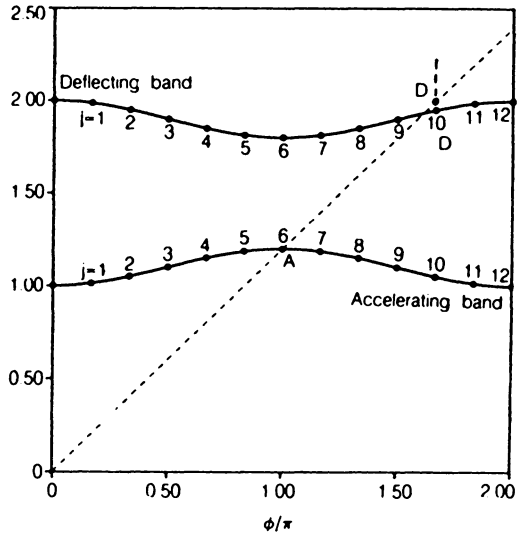

FIGURE 1 Accelerating and deflecting bands for a five-cavity structure with π-mode acceleration.

Here,

$$\psi = \frac{\omega_0 N_f L}{v} - j\pi = \frac{N_f L}{v}(\omega_D - \omega_{D'}) \qquad \text{(IV.A.3)}$$

is the slip of the *jth* mode of frequency $\omega_D/2\pi$ with respect to the beam bunch. The function $g(\psi)$, shown in Fig. 2, is normalized to have the value 1 at $\psi = \pi$, and has a maximum value of 1.05 at $\psi = 2.65$. For small coupling constant k, the

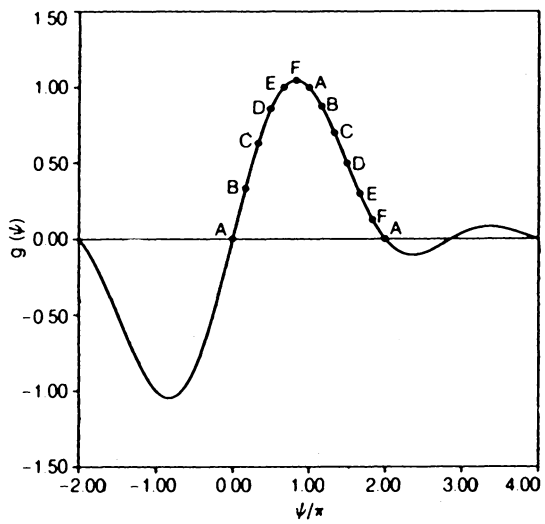

FIGURE 2 Slip function vs. slip angle for regenerative beam breakup.

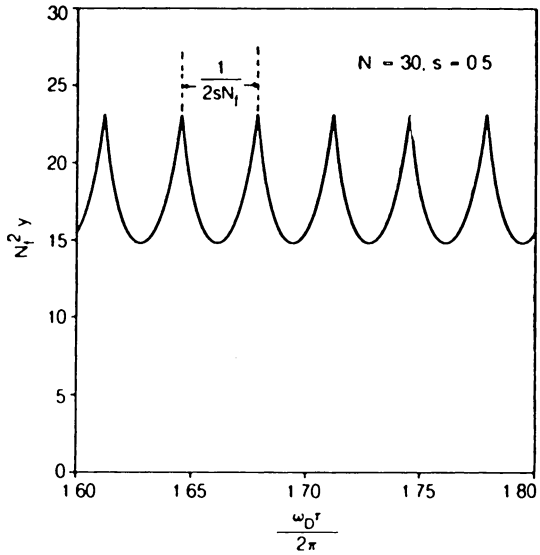

FIGURE 3 Regenerative-beam-breakup starting current as a function of deflecting mode frequency

deflecting band is approximately horizontal and the change in slip from one mode to the next is approximately π. The dominance of a single mode is then guaranteed by the sharpness of the function $g(\psi)$.

The main assumption of the foregoing model is that the width of each mode is small compared to the spacing between modes; that is,

$$\frac{\omega}{Q} \ll \frac{k\omega}{N_f}. \tag{IV.A.4}$$

If we change the frequency of the transverse band, the slip for a single mode, which is proportional to $\omega_D - \omega_{D'}$, will change rapidly. In particular, the dominant mode will rapidly give way to an adjacent mode whose slip is closest to $\psi = 2.65$. The variation of starting current with frequency will therefore have a scalloped character, such as that shown in Fig. 3, where the vertices correspond to the change in identification of the dominant mode.

We shall now examine the way in which the analysis of Sections II and III can be applied to the regenerative beam breakup limit.

b. Meaning of the Parameter x

In the previous section, we derived a universal curve for the starting current ($y = rQ/\omega\tau$) as a function of the coupling constant ($x = 1/kQ$). The derivation started as a departure from cumulative beam breakup for small coupling. The simulations confirm the universal curve's lack of dependence on the coupling constant k, particularly for all except the smallest values of x.

It is instructive to explore the meaning of the parameter $x = 1/kQ$. In the presence of coupling, a dispersion band exists which has a relative bandwidth k, and which has $N_f + 1$ distinct modes whose relative frequency separation is of order k/N_f except near the band edges. The relative frequency width of each mode is of order Q^{-1}. Thus, $x = 1/kQ > 1$ corresponds to the case where the width of each mode is larger than the width of the band and all modes are expected to participate simultaneously; this situation corresponds to cumulative beam breakup as $k \to 0$. For $x = 1/kQ < 1/N_f$, the width of each mode is smaller than the separation between modes, and only one mode is expected to participate (or possibly two modes). This is the regenerative beam breakup limit. For $1 < x < 1/N_f$, several modes will participate, and the situation will fall between these limits.

c. *Solution for Small x; Regenerative Beam Breakup*

As discussed above, the conditions appropriate to regenerative beam breakup are expected to apply for small x. In Appendix B we will demonstrate that the regenerative beam breakup limit given in Section IV.A can be derived from the beam breakup formalism in Section III.B. Specifically we will show that

$$y_{\text{RBBU}} \simeq \frac{15}{N_f^2} \tag{IV.C.1}$$

as $x \to 0$, is agreement with the result of Wilson.[6]

d. *Dependence on Frequency and on the Strength of the Coupling*

If the coupling k is very small, the dispersion curve is approximately horizontal. In this case the value of ψ in adjacent modes differs by π, as can be seen from Eq. (IV.A.3) where ω_D is the same for all deflective modes. The minimum starting current occurs at the frequency for which the slip ψ is approximately $5\pi/6$, corresponding to the point F in Fig. 2. The adjacent mode has a slip of approximately $11\pi/6$, corresponding to the point F' in Fig. 2, clearly corresponding to a higher starting current. As the frequency ω_D is decreased, the point F moves to the point E, corresponding to a slightly higher starting current; that is, lower $g(\psi)$. Once again the adjacent mode is not excited (point E'). As the frequency continues to decrease one progresses to point C, but now the adjacent mode at C' takes over, since $g(\psi)$ at C' is slightly larger than $g(\psi)$ at C. The starting current now begins to decrease, again reaching a minimum after the progression from C' to B' to A' to F. Thus the dependence of the starting current on frequency shown in Fig. 3 has a scalloped character, as the excitation jumps from one mode to the next. The frequency interval per scallop is clearly

$$\Delta\omega_D = \frac{\pi v}{N_f L}, \qquad \Delta(\omega_D \tau) = \frac{\pi}{s N_f}. \tag{IV.D.1}$$

If the coupling constant k is not negligible, it is clear from Fig. 1 that the difference in slip between adjacent modes is less than π if $d\omega/dk$ is positive, and greater than π if $d\omega/dk$ is negative. Where the difference in slip is less than π, the depth of the scallops is less than the factor 1.6 in Fig. 3 likewise, where the difference in slip is greater than π, the depth of the scallops is greater than the factor 1.6. This behaviour will be seen in simulations discussed later.

One final point regarding the preceding analysis: if the value of the coupling constant is sufficiently large, there will be multiple intersections between the deflecting band and the line OAD'. In this case the picture becomes far more complicated, and our universal curves will no longer be valid. This will occur for π-mode acceleration when k is of order

$$k_{\max} \sim \frac{2}{\pi} \frac{\omega_a}{\omega_D}, \tag{IV.D.2}$$

where $\omega_a/2\pi$ is the accelerating mode frequency.

V. GROWTH RATES

a. General Comments

We have shown that the presence of coupling between cavities leads to the existence of a starting current, above which the field amplitudes and transverse displacement grow exponentially. This may not be harmful if the beam pulse is short. For this reason it is often useful to be able to estimate the growth rate for the instability above the starting current.

b. Low Coupling Constant

The result in Section III can be used directly to obtain the growth rate when the coupling is small. Specifically, from Eqs. (III.B.6) and (III.B.8), the growth rate per pulse is

$$r_g = \exp\left[\frac{\omega\tau}{2Q}(\mathrm{Im}\,(q) - 1)\right]. \tag{V.B.1}$$

We calculated q for different values of N in Section III.C. For $N = 2$, we have $\mathrm{Im}\,(q) = v$, where v can easily be obtained from Eq. (III.C.3). For higher N the result in Eq. (III.D.5) represents the leading term for large $|x|$, namely

$$\mathrm{Im}\,(q) = (2v/|x|)^{1/2} \cos\frac{\pi}{N+1}\begin{cases}\cos(\theta/2), & x>0\\ \sin(\theta/2), & x<0\end{cases}. \tag{V.B.2}$$

This estimate is for the root with the greatest growth rate, although there is some evidence from numerical work that the roots occasionally cross as x is changed continuously.

c. Regenerative Beam Breakup Limit

In order to estimate the growth rate in the regenerative beam breakup limit, we need to determine the dependence of the impulse to the cavity field on the entering phase ωt_0 of the beam bunch. This is most easily done by calculating the trajectory $x(z)$ for each beam bunch in the cavity and then calculating the field impulse. The field impulse is proportional to

$$\int_0^L x(z) \frac{\partial E_z}{\partial x}(z, t)\, dz, \tag{V.C.1}$$

where $\partial E_z/\partial x$ is evaluated at $x = y = 0$, $t = t_0 + z/v$. Rapidly oscillating terms are neglected. The final result is

$$\operatorname{Im} q = \frac{2yN_f^2}{\pi^3}[g(\psi) + h(\psi) \sin(2\omega t_0 - \psi)], \tag{V.C.2}$$

where $g(\psi)$ is given in Eq. (B.15), and

$$h(\psi) = \frac{\psi - \sin\psi}{4(\psi/\pi)^3}. \tag{V.C.3}$$

The field amplitude is then modified by the factor

$$A + B\cos\chi_i \tag{V.C.4}$$

as a result of the transit of the *ith* beam bunch, where

$$A = 1 + \frac{\omega\tau}{2Q}\left[\frac{2yN_f^2}{\pi^3} g(\psi) - 1\right] \tag{V.C.5}$$

$$B = \frac{\omega\tau}{2Q}\left[\frac{2yN_f^2}{\pi^3} h(\psi)\right]. \tag{V.C.6}$$

The average growth rate r_g will then be given by the product over many beam bunches:

$$r_g^M = \prod_{i=1}^{M} (A + B\cos\chi_i). \tag{V.C.7}$$

If we average over χ_i, which is related to the entering phase, we can write

$$\ln r_g = \frac{1}{2\pi}\int_0^{2\pi} d\chi \ln(A + B\cos\chi). \tag{V.C.8}$$

The integral can be evaluated by conversion to a contour integral over $z = e^{i\chi}$, where the contour encloses the branch points of the logarithm at

$$z = 0 \quad \text{and} \quad z = \frac{-A + (A^2 - B^2)^{1/2}}{B}.$$

The final result is

$$r_g = \frac{A + (A^2 - B^2)^{1/2}}{2}. \tag{V.C.9}$$

As a check, the starting current is given by $r_g = 1$, or

$$A - 1 = \frac{B^2}{4}. \tag{V.C.10}$$

This corresponds to

$$\frac{2yN_f^2 g(\psi)}{\pi^3} = 1 + \frac{\omega\tau}{2Q}\left[\frac{yN_f^2}{\pi^3} h(\psi)\right]^2, \tag{V.C.11}$$

which agrees with Eq. (B.16) for values of yN_f^2/π^3 of order 1. In the limit

$$\frac{\omega\tau}{2Q}\frac{2yN_f^2}{\pi^3} = \frac{rN_f^2}{\pi^3} \gg 1, \tag{V.C.12}$$

the growth rate is

$$r_g = \frac{rN_f^2}{2\pi^3}[g(\psi) + (g^2(\psi) - h^2(\psi))^{1/2}], \quad g(\psi) > h(\psi), \tag{V.C.13}$$

or

$$r_g = \frac{rN_f^2}{2\pi^3} h(\psi), \quad g(\psi) < h(\psi). \tag{V.C.14}$$

VI. SIMULATIONS

a. Low Coupling Constant

The parameters which are used in the simulations are similar to those used in our earlier papers.[1,3,4] Specifically we use the nominal values

$$r = 2.88 \times 10^{-3} \qquad \omega\tau/2\pi = 1.70 \qquad Q = 1000 \qquad N_f = 30,$$
$$s = 0.5 \ (\pi\text{-mode acceleration}) \tag{VI.A.1}$$

although we will vary these parameters as we proceed.

Figure 4a shows the ratio of the displacement to the initial displacement for a single displaced pulse, as a function of M, in the absence of coupling. This shows the general behavior of cumulative beam breakup discussed in detail in an earlier paper. In Figs. 4b, 4c, 4d, 4e, 4f, and 4g we show this ratio for the values of $k = 0.0040$, 0.0045, 0.0050, -0.0010, -0.00144, and -0.0015. Clearly the starting current

$$y = \frac{rQ}{\omega\tau} \tag{VI.A.2}$$

is reached for positive k at about 0.0045 and for negative k at about -0.0015. This is consistent with Eq. (III.A.17) where the sign of k is critical.

In order to test Eq. (III.A.17) more quantitatively, we compute an equivalent

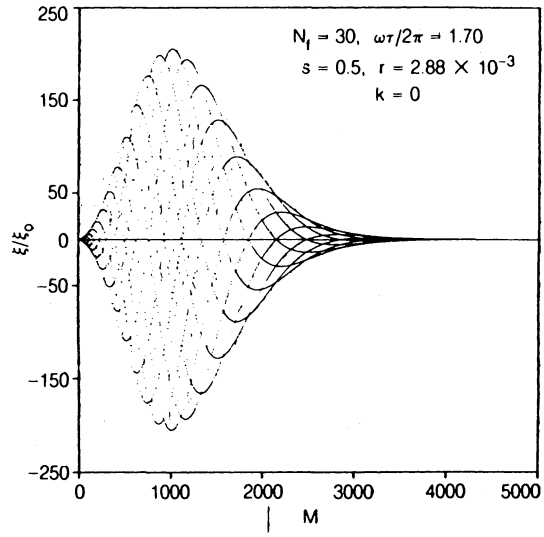

FIGURE 4a | Displacement vs. bunch number for cumulative beam breakup without coupling.

exponent from the envelope of the simulations. Specifically, we compute

$$w(k) = \ln \frac{|\xi|_{\max}}{\xi_0} \qquad \text{(VI.A.3)}$$

and plot $w(k) - w(0)$ against $r^{1/3} N^{-1/3} M^{4/3}$ for the different values of k or ε. The result is shown in Fig. 5, where the linear behavior, with slope proportional to k or ε, is clearly shown.

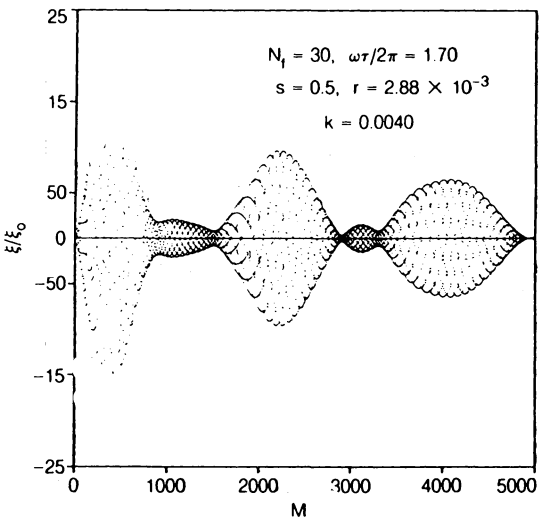

FIGURE 4b | Displacement vs. bunch number for cumulative beam breakup with coupling, $k = 0.0040$.

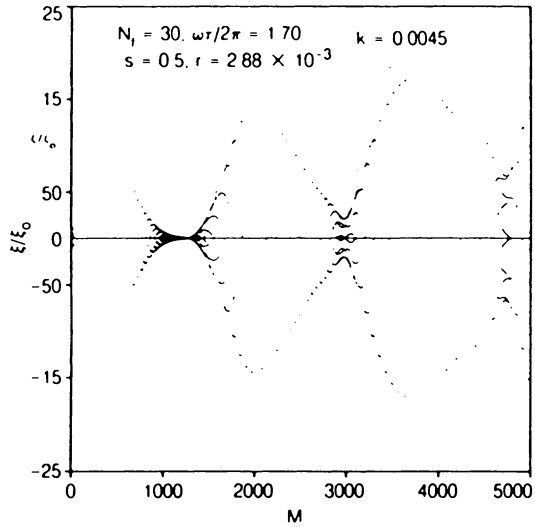

FIGURE 4c Displacement vs. bunch number for cumulative beam breakup with coupling, $k = 0.0045$.

In order to test the validity of Eq. (III.A.16), we compute

$$\frac{w(k) - w(0)}{r^{1/3}M^{1/3}} \tag{VI.A.4}$$

and plot it against $(N + \varepsilon M)^{2/3}$. The result is shown in Fig. 6 for $k = \pm 0.01$, where

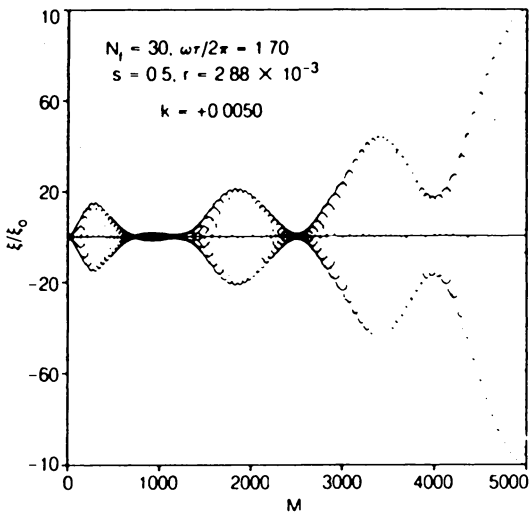

FIGURE 4d Displacement vs. bunch number for cumulative beam breakup with coupling, $k = 0.0050$.

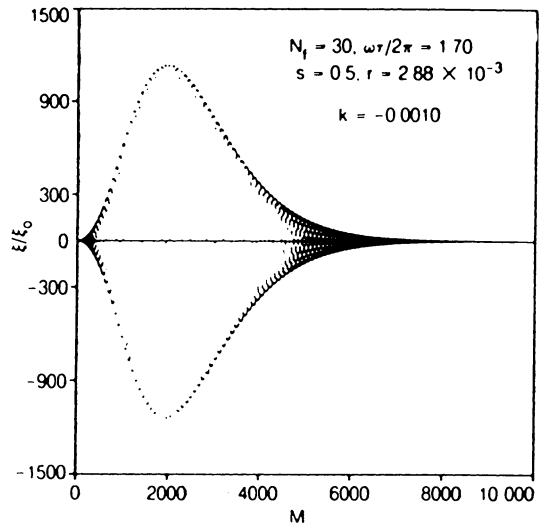

FIGURE 4e Displacement vs. bunch number for cumulative beam breakup with coupling, $k = -0.00100$.

it appears that Eq. (III.A.16) is confirmed for positive ε (negative k, because $\sin\theta$ is negative in Eq. (III.A.14)), but not for negative ε. The slope of the straight line for positive ε is 1.1, in approximate agreement with $3\sqrt{3}/4$ in Eq. (III.A.16). But Eq. (III.A.16) does not appear to be valid for negative ε for the reasons discussed in Section III.E and Appendix B.

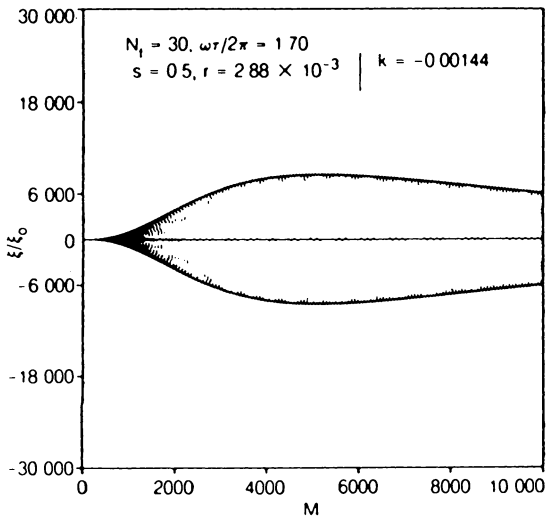

FIGURE 4f Displacement vs. bunch number for cumulative beam breakup with coupling, $k = -0.00144$.

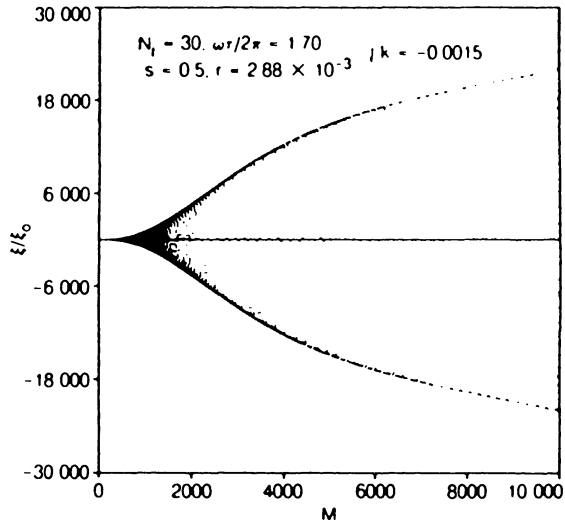

FIGURE 4g Displacement vs. bunch number for cumulative beam breakup with coupling, $k = -0.00150$.

b. Starting Current vs. x

Having established the validity of the low-k analysis, we now compute the starting current. The method used is that described at the start of Section II.C. For pedagogical purposes, however, we will assume that we are dealing with the

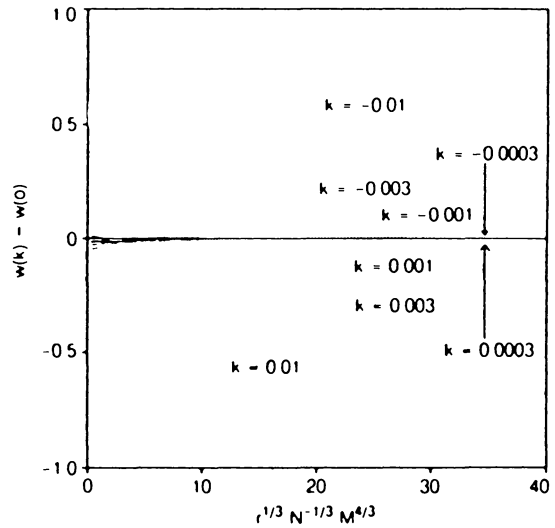

FIGURE 5 Test of the $M^{4/3}$ behavior of the exponent in cumulative beam breakup with small coupling.

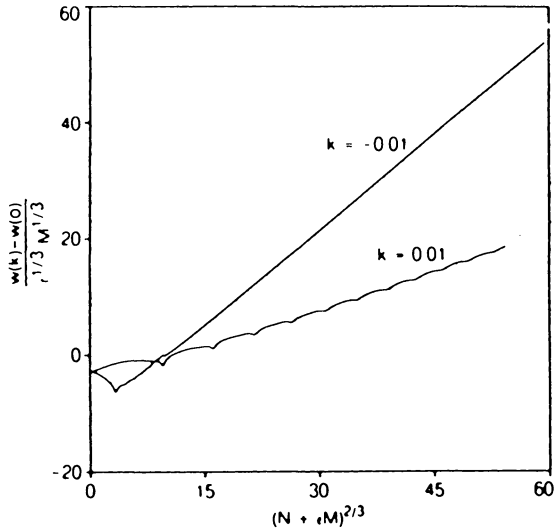

FIGURE 6 Test of the $(M + \varepsilon N)^{2/3}$ behavior of the exponent in cumulative beam breaking with small coupling.

smoothed difference equations (II.C.3) and (II.C.4), written in the form

$$f(M+s) = \mathfrak{M} f(M-s) \qquad \text{(VI.B.1)}$$

where f is an N_f-dimensional vector and $\mathfrak{M}$ is an $N_f \times N_f$ dimensional matrix whose coefficients are contained in Eqs. (II.C.3) and (II.C.4). We are trying to

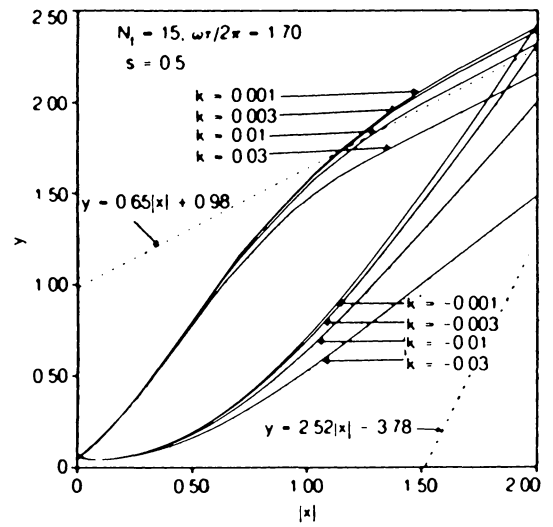

FIGURE 7 Starting current y vs. coupling parameter x for a 15-cavity structure, including linear asymptotes.

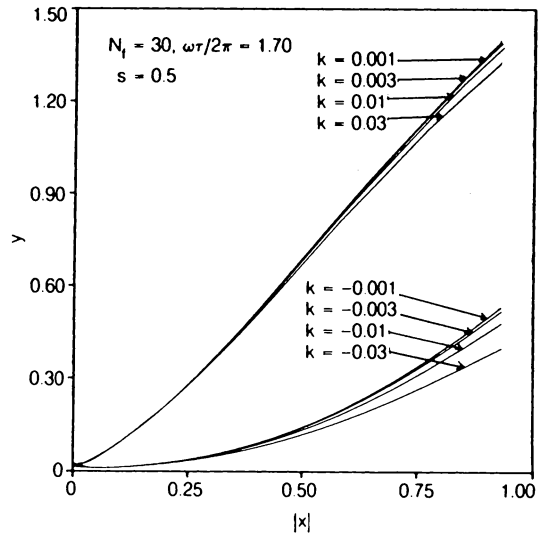

FIGURE 8 Starting current y vs. coupling parameter x for a 30-cavity structure.

obtain the behavior of f for large M. Clearly, repeated application of $\mathfrak{M}$ to an arbitrary starting vector will filter out all but the mode with the largest growth rate, and we will be able to determine this growth rate (equivalent to Re (p) or Im (q) in Eq. (III.B.8)). We thus can obtain the starting current at which the growth rate of f exceeds the decay rate due to Q.

This procedure, as mentioned above, is applied with the difference equations and propagator described at the start of Section II.C in order to obtain the

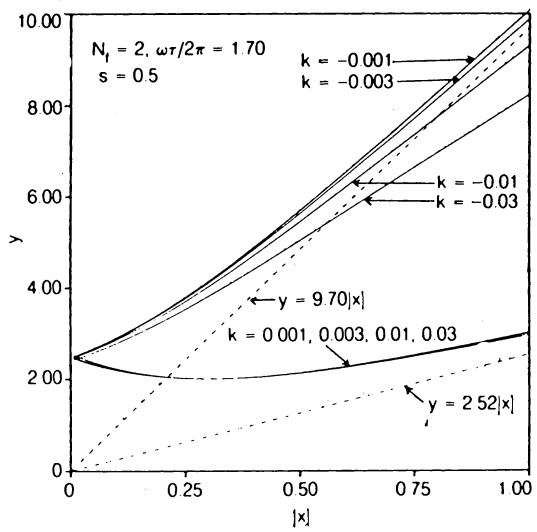

FIGURE 9 Starting current y vs. coupling parameter x for a 2-cavity structure, including linear asymptotes.

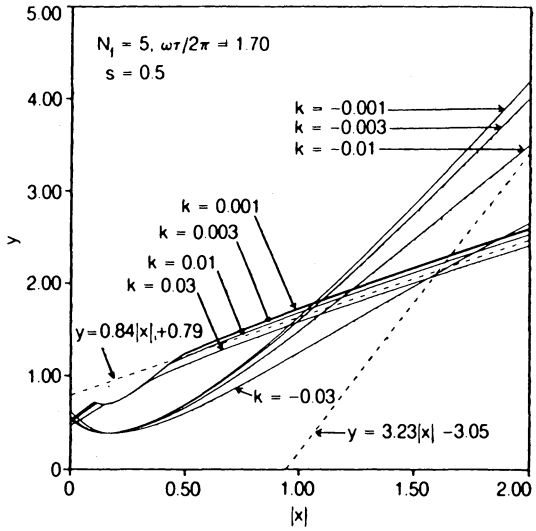

FIGURE 10 Starting current y vs. coupling parameter x for a 5-cavity structure, including linear asymptotes.

starting current. The results are shown in Fig. 7 ($N_f = 15$) and Fig. 8 $N_f = 30$). In Figs 7 and 8, the starting current is given by $y(=rQ/\omega\tau)$ as a function of the parameter $|x| = 1/|k|Q$; we compute it for several different values of k. (Variation of x is obtained by varying Q.) The quadratic behavior of y vs. x is evident for negative k (positive ε) for values of $x < 1$, but it appears that the curve becomes more linear for $x > 1$. The approach to linearity predicted in Eq. (III.D.10), is shown in fig. 7 as the asymptotes plotted as dashed lines.

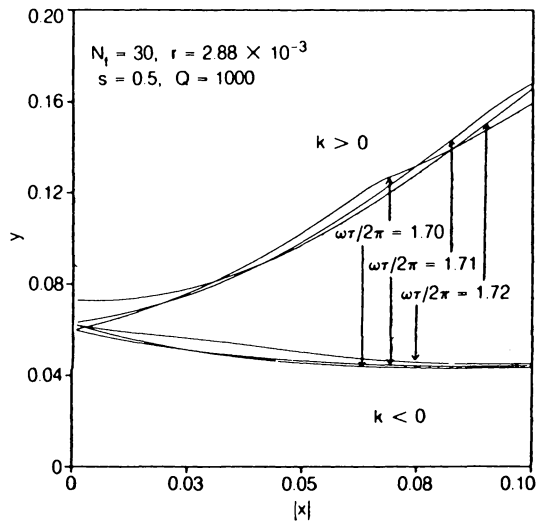

FIGURE 11 Variation of starting current with deflecting-mode frequency.

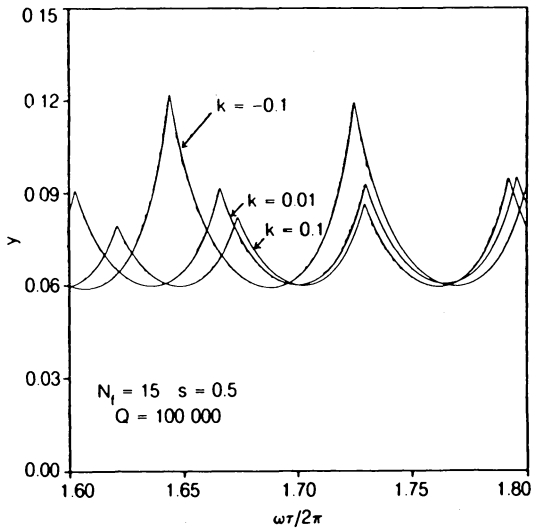

FIGURE 12 Starting current for regenerative beam breakup as a function of deflecting-mode frequency for different coupling constants.

The approach to linearity is even more clearly visible in Fig. 9 ($N_f = 2$) and 10 ($N_f = 5$), where the asymptotes Eq. (IIILD.10) are again shown as dashed lines. Note the crossing of the curves for $k < 0$ and $k > 0$ for $N_f \geq 5$.

c. *Regenerative Beam Breakup Limit*

In Fig. 11 we plot the starting current in the high-Q, low-x region for different values of the deflecting mode frequency. The sensitive dependence of the starting current on the frequency reflects our discussion in Section IV.E concerning the slip of the beam bunch with respect to the individual tank modes. To illustrate this better, we plot the regenerative beam breakup starting current ($Q \to \infty$, $r \to 0$) as a function of $\omega\tau/2\pi$ in Fig. 12 for different values of k. The scalloped behavior is clear, as is the dependence of the depth and width of the scallops for different k.

VII. SUMMARY

We have started with the difference equations for *cumulative beam breakup* (CBBU) and have modified them to include coupling between adjacent cells in the deflecting mode to obtain the difference equations in Eqs. (II.C.3) and (II.C.4). To obtain the effect of small coupling, we approximated these by the differential equations in Eqs. (II.C.7) and (III.A.9), and from these obtained the modification to the CBBU transient exponent for small k given in Eqs. (III.A.16) and (III.A.17). Figures 5 and 6 show the confirmation of these results, obtained

by using the simulations. Figure 4a–4g show the dramatic effect of a small coupling on the CBBU transient.

The coupled system in Eqs. (II.C.3) and (II.C.4) is examined for finite N and shown to correspond to the existence of a starting current above which there is a runaway excitation. Values of the starting current for different parameters are obtained from a numerical procedure which solves for the roots of an $N \times N$ determinantal equation. The analysis is Sections (II.B), (II.C), and (III.D) suggests that the starting current, in the form of $y = rQ/\omega\tau$, is approximately a universal function of the coupling constant, in the form of $|x| = 1/|k|Q$. Results are shown in this form in Figs 7–10 for various values of N. These are the results which should be useful in making estimates for particular linac configurations.

Finally, a physical interpretation of the parameter $|x|$ is developed; it corresponds to the relative width of the multi-cell modes of excitation Q^{-1}, their relative separation k/N_f, and the deflecting band relative width k. It is shown that $|x| \gg 1$ corresponds to CBBU and that $|x| \ll 1$ corresponds to RBBU. The usual results for RBBU[5] are derived from our formalism in the small x approximation. The transition region, for which $|x|$ is between $1/N_f$ and 1, is the one for which the universal curves in Figs. 7–10 appear to apply and will be most useful.

VIII. ACKNOWLEDGMENT

The authors are grateful for the hospitality of the Accelerator Technology (AT) Division at Los Alamos National Laboratory, where some of this work was done, and to Richard K. Cooper for suggesting this study and for many stimulating conversations during the course of the work.

REFERENCES

1. R. L. Gluckstern, R. K. Cooper, and P. J. Channell, *Part. Accel.* **16,** 125 (1985).
2. V. K. Neil, L. S. Hall, and R. K. Cooper, *Part. Accel.* **9,** 213 (1979).
3. R. L. Gluckstern, F. Neri, and R. K. Cooper, *Part. Accel.* **23,** 37 (1988).
4. R. L. Gluckstern, F. Neri, and R. K. Cooper, *Part. Accel.* **23,** 53 (1988).
5. Y. Y. Lau, "Asymptotic Growth of Cumulative and Regenerative Beam Breakup Instabilities," NRL Memo Report 6237 (1988), discusses asymptotic growth and group velocity under more general circumstances.
6. See, for example, P. B. Wilson, *Proceedings* of the Fermilab Summer School on Particle Accelerators, p. 450 (1981); R. H. Helm and G. A. Loew, *Linear Accelerators,* edited by P. Lapostille and A. Septier, John Wiley and Sons, p. 173 (1970).

APPENDIX A

Validity of Quadratic Behavior for Large N

In order to understand the validity of Eq. (III.A.20), we explore the derivation for large N by starting with Eq. (III.A.12), with $z(N, M)$ written in the form

given in Eq. (III.B.1), namely

$$z(N, M) = \frac{r}{2i} \sum_{j=1}^{N} jU(N-j, M). \tag{A.1}$$

(We have dropped the tilde in $\tilde{z}(N, m)$ and $U(N, M)$.) For large N we will rewrite Eq. (A.1) as

$$z(N, M) = \frac{r}{2i} \sum_{m=0}^{\infty} \frac{(-1)^m}{m!} \frac{\partial^m U}{\partial N^2} \sum_{j=1}^{\infty} j^{m+1} \cong \frac{rN^2}{2i} U(N, M)F, \tag{A.2}$$

where

$$F \equiv \frac{1}{U} \sum_{m=0}^{\infty} \frac{(-1)^m N^m}{(m+2)m!} \frac{\partial^m U}{\partial N^m}. \tag{A.3}$$

We now assume that the exponent for $U(N, M)$ and $Z(N, M)$ has the form suggested in Eq. (III.A.16), namely

$$ar^{1/3} M^{1/3} (N + \varepsilon M)^{2/3}, \tag{A.4}$$

where a is a complex parameter to be determined later. As before, we take derivatives of the exponent only, and obtain

$$\frac{1}{U} \frac{\partial^m U}{\partial N^m} \cong \left(\frac{1}{U} \frac{\partial U}{\partial N} \right) = \left[\frac{2a}{3} r^{1/3} \left(\frac{M}{N + \varepsilon M} \right)^{1/3} \right]^m. \tag{A.5}$$

Thus we can write F as

$$F = F(q) \equiv \sum_{m=0}^{\infty} \frac{(-1)^m q^m}{(m+2)m!} \tag{A.6}$$

where

$$q = \left(\frac{2a}{3} \right) r^{1/3} N \left(\frac{M}{N + \varepsilon M} \right)^{1/3}. \tag{A.7}$$

Multiplying Eq. (A.6) by q^2 and then differentiating with respect to q leads to

$$\frac{d}{dq} [q^2 F(q)] = \sum_{m=0}^{\infty} \frac{(-1)^m q^{m+1}}{m!} = qe^{-q}, \tag{A.8}$$

from which we obtain

$$q^2 F(q) = \int_0^q qe^{-q}\, dq. \tag{A.9}$$

If we now explore the limit for large N, we obtain

$$F(q) \cong \frac{1}{q^2}, \quad z(N, M) = \frac{rN^2}{2i} \frac{U(N, M)}{q^2} \tag{A.10}$$

provided that $\mathrm{Re}\,(q) > 0$.

The first equation in Eq. (III.A.12) assuming the same exponential form for $U(N, M)$, leads to the condition

$$\left(\frac{a}{3} \right) r^{1/3} \frac{(N + \varepsilon M)^{2/3}}{M^{2/3}} = \frac{rN^2}{2iq^2} = \frac{9}{8a^2} \frac{r}{i} \left(\frac{N + \varepsilon M}{M} \right)^{2/3} \frac{1}{r^{2/3}}, \tag{A.11}$$

which is correct provided that

$$a^3 = \frac{27}{8i}, \qquad a = \tfrac{3}{2}(e^{-\pi i/6}, e^{\pi i/2}, e^{-5\pi i/6}). \tag{A.12}$$

Let us now explore the condition $\mathrm{Re}\,(q) > 0$. For positive ε, this leads, from Eq. (A.7), to $\mathrm{Re}\,a > 0$, or

$$\mathrm{Re}\,a = \frac{3\sqrt{3}}{4} \quad \text{for} \quad \varepsilon > 0, \tag{A.13}$$

consistent with the exponent derived in Eq. (III.A.17). For negative ε however, the large[1] M limit for q is

$$q = \left(\frac{2a}{3}\right) r^{1/3} N \left(\frac{M}{N + \varepsilon M}\right)^{1/3} \to -\frac{2a}{3} \frac{r^{1/3} N}{|\varepsilon|^{1/3}}, \tag{A.14}$$

thus requiring

$$\mathrm{Re}\,a = -\frac{3\sqrt{3}}{4} \quad \text{for} \quad \varepsilon > 0, \tag{A.15}$$

implying an exponent

$$e_k = -\frac{M\omega\tau}{2Q} - \frac{3\sqrt{3}}{4} r^{1/3} M^{1/3} (N + \varepsilon M)^{2/3} \tag{A.16}$$

instead of the one in Eq. (III.A.16). For large M, this does not correspond to a runaway displacement, and the starting current corresponding to Eq. (III.A.20) or Eq. (III.D.11) is therefore valid for positive ε, but not for negative ε. This is consistent with the simulations, as discussed earlier.

APPENDIX B

Starting Current for Small x; Regenerative Beam Breakup

In this appendix, we explore the small x limit and show that the results agree with those previously derived for regenerative beam breakup. Our starting point will be Eq. (III.B.13), with the change of variable

$$D_N = (aa^*)^{N/2} F_N = (2x)^{-N} F_N \tag{B.1}$$

leading to

$$F_{N+1} + 2\cos\phi F_N + F_{N-1} = g_N \tag{B.2}$$

where

$$g_N = 2yx \sum_{m=1}^{N-1} (-1)^m m e^{-im\theta} F_{N-m} \tag{B.3}$$

and

$$qx \equiv -\cos\phi. \tag{B.4}$$

The sign of $\cos\phi$ is chosen so that ϕ is the phase advance of the field from one

cell to the next. For small x, y will be finite and g_N can be treated as a small perturbation.

The solution to Eq. (B.2) with $g_N = 0$ is readily obtained. It is

$$F_N = (-1)^N \frac{\sin (N+1)\phi}{\sin \phi}, \qquad N \geqslant -1 \tag{B.5}$$

which is consistent with Eq. (III.B.14) and which now can be used on the right side of Eq. (B.3). The solution to Eq. (B.2) can be readily seen to be

$$F_N = (-1)^N \frac{\sin (N+1)\phi}{\sin \phi} + \Delta F_N, \tag{B.6}$$

where

$$\Delta F_N = -\frac{(-1)^N}{\sin \phi} \sum_{l=0}^{N} g_l (-1)^l \sin (N-l)\phi. \tag{B.7}$$

Using Eqs. (IV.B.3) and (IV.B.5), we can write

$$\begin{aligned} \Delta F_N &= -\frac{2yx(-1)^N}{\sin^2 \phi} \sum_{l=0}^{N} \sum_{m=0}^{l} m e^{im\theta} \sin (l-m+1)\phi \sin (N-l)\phi \\ &= -\frac{yx(-1)^N}{\sin^2 \phi} \sum_{m=0}^{N} m e^{-im\theta} \sum_{l=m}^{N} [\cos (2l-m-N+1)\phi - \cos (N-m+1)\phi]. \end{aligned} \tag{B.8}$$

We shall assume that, for large N, the first term in the brackets [ ] will oscillate rapidly with l and can be neglected, while the second term is independent of l. We can therefore write

$$\Delta F_N \cong \frac{yx(-1)^{j+N}}{2 \sin^2 \phi} \sum_{m=0}^{N} (-1)^m m(N-m+1)[e^{-im(\theta-\phi)} + e^{-im(\theta+\phi)}], \tag{B.9}$$

where we have used the approximate value $\phi \cong j\pi(N_f + 1)$ on the right side of Eq. (B.8).

Before proceeding further, we will apply the condition for the starting current, namely $F_{N_f} = 0$. From Eq. (B.6), the solution for ϕ is then given by

$$\sin (N_f + 1)\phi = -\sin \phi (-1)^N \Delta F_{N_f}$$

or

$$\phi \cong \frac{j\pi}{N_f + 1} - (-1)^{N_f + j} \frac{\sin \phi \Delta F_{N_f}}{N_f + 1}\bigg|_{\phi = j\pi/(N_f+1)}. \tag{B.10}$$

This leads to

$$q = -\frac{\cos \phi}{x} \cong -\frac{\cos \dfrac{j\pi}{N_f + 1}}{x} - (-1)^{N+j} \frac{\sin^2 \phi \Delta F_{N_f}}{(N_f + 1)x}\bigg|_{\phi = j\pi/(N_f+1)} \tag{B.11}$$

The starting current condition in Eq. (III.B.12), namely $\mathrm{Im}\,(q) = 1$, then

becomes

$$-(-1)^{N_f+j}\frac{\sin^2\phi}{(N_f+1)x}\,\mathrm{Im}\,\Delta F_{N_f}=1,$$

or

$$\mathrm{Im}\sum_{m=0}^{N_f} m(N_f+1-m)[e^{-im(\theta-\phi)}+e^{-im(\theta+\phi)}]=-\frac{2(N_f+1)}{y}. \tag{B.12}$$

The lowest value of the starting current, y, therefore corresponds to the largest value of the left side of Eq. (B. 12). This will occur for small $|\theta-\phi|$, since otherwise there will be cancellation due to the oscillation of the exponential term. If we write

$$\psi=N_f(\theta-\phi), \tag{B.13}$$

replace the sum in Eq. (B.12) by an integral, and neglect the rapidly oscillating term in $(\theta+\phi)$, we obtain

$$\mathrm{Im}\left\{\int_0^1 du(1-u)ue^{-i\psi u}\right\}\cong-\frac{2}{N_f^2y}. \tag{B.14}$$

The integral on the left side is readily evaluated to be $-4g(\psi)/\pi^3$, where

$$g(\psi)=\frac{1-\cos\psi-\dfrac{\psi}{2}\sin\psi}{2(\psi/\pi)^3}. \tag{B.15}$$

One therefore obtains for the starting current

$$y=\frac{\pi^3}{2N_f^2g(\psi)}, \tag{B.16}$$

in agreement with the result in Eq. (IV.A.1).

The parameter ψ can be written for large N_f, using Eqs. (II.C.5) and (II.B.5), as

$$\psi=N_fs\omega\tau-j\pi=\frac{\omega}{c}N_fL-j\pi \tag{B.17}$$

which is the slip of the beam bunch with respect to the wave corresponding to the jth mode in a tank of N_f cavities, as explained in Section IV.A. Equation (B. 16), which is that derived by Wilson,[6] implies that the lowest starting current occurs if the slip ψ has the value 2.65, for which

$$y_{\mathrm{RBBU}}\cong\frac{15}{N_f^2}\quad\text{as}\quad x\to 0. \tag{B.18}$$

What we have accomplished here is the derivation of the starting current for regenerative beam breakup, starting with Eq. (III.B.9), which applies in general for coupled cavities.